Research Square

Preprints are preliminary reports that have not undergone peer review.
They should not be considered conclusive, used to inform clinical practice,
or referenced by the media as validated information.

Perioperative urine metabolomic reprogramming associated with skeletal muscle wasting in cardiac valve surgery

Chengyao Xu
Shanghai University of Sport
Shidong Liu
First Hospital of Lanzhou University
Dan Guo
First Hospital of Lanzhou University
Haiyi He
Shanghai University of Sport
Bing Song
First Hospital of Lanzhou University
Xin Xu
xuxin@sus.edu.cn

Shanghai University of Sport

Article

Keywords: ICU-acquired weakness, Cardiac valve surgery, Skeletal muscle wasting, Untargeted metabolomics, ERAS, Nutritional prehabilitation

Posted Date: September 25th, 2026

DOI: https://doi.org/10.21203/rs.3.rs-10902993/v1

License: This work is licensed under a Creative Commons Attribution 4.0 International License.
Read Full License

Additional Declarations: No competing interests reported.

Abstract

Background

To define perioperative urine metabolomic reprogramming linked to skeletal muscle wasting in cardiac valve surgery patients under an Enhanced Recovery After Surgery (ERAS) protocol, and to identify actionable nutritional targets and non-invasive candidates for ICU-acquired weakness (ICU-AW) risk stratification.

Methods

This prospective observational study enrolled 93 valvular heart disease patients (aged 18–75, NYHA I–III) undergoing elective valve surgery under ERAS, with a randomly sampled untargeted metabolomics subcohort (n = 28). Urine was collected at admission and ICU discharge and analyzed by SCIEX Zeno TOF 7600 (HILIC/C18), with probabilistic quotient normalization and osmolality verification. Limb circumferences served as validated surrogates for muscle mass; ICU-AW risk was operationalized via these surrogates rather than the MRC sum score. Paired t-tests with FDR correction, Spearman correlation, and KEGG/GO/STITCH enrichment were applied.

Results

ERAS enabled efficient recovery (median ICU stay 44 h, mechanical ventilation 8.9 h), yet CRP surged from 3.95 to 63.34 mg/L postoperatively and stayed elevated at discharge, and calf circumferences fell below sex-specific sarcopenia cut-offs. Metabolomics identified 234 and 202 differential metabolites in positive and negative modes. KEGG enrichment highlighted 21 pathways across amino acid, lipid, cofactor/vitamin, and bile acid–gut-liver metabolism. Twenty urinary metabolites correlated significantly with discharge calf circumference ($|r|>0.38$); acacetin 7-glucuronide and gravacridonechlorine showed the strongest positive correlations, while glycitein and pummeline were negatively correlated. Mechanistic enrichment converged on hypoxia, oxidative stress, and the PI3K-Akt/FoxO axis.

Conclusion

A "sarcopenia–inflammation–metabolic rewiring" triad drives ICU-AW in valve surgery. Perturbed tryptophan, histidine, and vitamin B6 metabolism form a self-perpetuating loop of inflammation, mitochondrial dysfunction, and proteolysis, representing actionable targets for precision nutritional prehabilitation.

1 Introduction

ICU-acquired weakness (ICU-AW) affects 25–60% of patients requiring prolonged mechanical ventilation and causes nearly 1 million new cases annually, serving as a prevalent neuromuscular complication and independent predictor of adverse outcomes after cardiac valve surgery.(1, 2) It prolongs mechanical ventilation, extends ICU/hospital stays, impairs long-term function, and elevates mortality.(3, 4) Cardiac valve surgery imposes modifiable perioperative stressors — cardiopulmonary bypass-induced systemic inflammation, immobilization, nutritional depletion, and metabolic derangement — that converge to drive ICU-AW. Skeletal muscle atrophy is the cardinal phenotypic hallmark, with measurable loss beginning within days of ICU admission (pooled first-week reduction > 15%; meta-analytic mean ~ 1.5–2.0%/day).(5) At the molecular level, ICU-AW arises from sustained inflammation and glucocorticoid excess activating catabolic signaling, oxidative stress and mitochondrial dysfunction impairing bioenergetics, and hyperactivation of the ubiquitin-proteasome system coupled with dysregulated autophagy mediating preferential myosin loss.(5, 6) Emerging evidence implicates lipid and cholesterol homeostasis, extending pathogenic models beyond classic proteolysis.(1) A temporally resolved mechanistic framework across the ICU-AW trajectory remains undefined—particularly in cardiac valve surgery patients, where bypass-induced inflammation may reweight dominant drivers. Addressing this gap is a prerequisite for mechanism-informed early identification and precision intervention; structured risk stratification and early targeted intervention are therefore imperative in this cohort.

Malnutrition and impaired protein–energy homeostasis are increasingly recognised as central, modifiable drivers of ICU-acquired weakness (ICU-AW). Although nutritional support is well established in attenuating muscle catabolism, the precise metabolic pathways linking peri-operative nutritional status to muscle wasting in cardiac surgery remain poorly defined. Emerging evidence implicates perturbations in amino-acid catabolism, lipid and cholesterol homeostasis, and vitamin-cofactor metabolism—extending pathogenic models beyond classical proteolysis and opening avenues for precision nutritional intervention. Patients undergoing cardiac valve surgery represent a particularly informative cohort: underlying valvular pathology frequently coexists with pre-existing sarcopenia and malnutrition, while cardiopulmonary bypass triggers a systemic inflammatory response that may reweight the dominant metabolic drivers of wasting. Closing this mechanistic gap is a prerequisite for mechanism-informed early identification and targeted nutritional therapy.

Metabolomics captures low-molecular-weight metabolites that reflect underlying pathophysiology. In critically ill patients, circulating creatinine, glycerophospholipids, and acylcarnitines have been shown to correlate with muscle mass and muscle loss, as well as with mitochondrial and catabolic stress.(7, 8) Within cardiac-valve-surgery cohorts, peri-operative metabolomics enables characterisation of the metabolic states that coincide with ICU-AW–associated atrophy and informs the discovery of candidate biomarkers. In this study, we integrated untargeted metabolomics with objectively quantified muscle loss and functional weakness to define temporal metabolite trajectories aligned with wasting progression. We identified candidate metabolite clusters enriched in amino-acid catabolism, acylcarnitine/fatty-acid-oxidation intermediates, and redox-linked species that discriminated progressive from limited wasting, and derived a preliminary metabolic signature for risk stratification. ICU-AW risk was operationalised through serial limb-circumference–derived muscle-mass surrogates and

biomarker–metabolite correlations, rather than the MRC sum score—the gold-standard bedside diagnostic, in which a total score < 48 defines ICU-AW. This constitutes a limitation: our findings characterise the catabolic/mass-loss phenotype that overlaps with, but is not synonymous with, clinically defined ICU-AW.

2 Materials and methods

2.1 Study design and participants

We enrolled 93 valvular heart disease patients (aged 18–75, NYHA I–III) undergoing elective valve repair/replacement under ERAS, with a randomly sampled metabolomics subcohort (n = 28). No external control was recruited; each patient served as their own baseline (preoperative vs. ICU discharge). Sample size for the metabolomics subcohort was determined by feasibility and aligned with published exploratory untargeted metabolomics studies; a post-hoc power estimation indicated 80% power to detect metabolites with effect size $|r|>0.5$ at $\alpha = 0.05$. Perioperative rehabilitation was risk-stratified and dynamically adjusted. The study was approved by the Medical Ethics Committee of The First Hospital of Lanzhou University (No. LDYYLL2026-526) and conducted per the Declaration of Helsinki with written informed consent from all participants. (Table.1)

2.2 Muscle mass assessment

Serial limb circumferences were measured as previously validated surrogates for skeletal muscle mass. Calf circumference was measured with a non-elastic tape at 10 cm proximal to the medial malleolus, with the patient in supine position after 10 minutes of rest, recorded to the nearest 0.1 cm. Sex-specific cut-offs for sarcopenia were applied (men < 34 cm, women < 33 cm). ICU-AW risk was operationalized through limb-circumference-derived surrogates rather than the MRC sum score

2.3 Urine collection and metabolomics

Urine was collected at admission and ICU discharge. Mid-stream urine samples were immediately aliquoted and stored at − 80°C pending analysis. Samples were analyzed by untargeted metabolomics (SCIEX Zeno TOF 7600; HILIC/C18). Urinary metabolite intensities were normalized using probabilistic quotient normalization (PQN) with osmolality-based verification to account for hydration variability; given the low muscle mass in the study population, creatinine-only normalization was avoided to prevent bias. Quality control (QC) pooled samples were injected at regular intervals to monitor instrument stability.

2.4 Statistical analysis

Data were analyzed using SPSS and R. Paired t-tests with Benjamini-Hochberg false discovery rate (FDR) correction ($p < 0.05$, fold change > 1.5 or < 0.67, VIP > 1) identified differential metabolites. Metabolite identification was assigned confidence levels per the Metabolomics Standards Initiative (MSI). Spearman correlation between postoperative urinary metabolome and discharge calf circumference was performed with FDR correction. KEGG pathway enrichment was conducted on metabolite sets using a

threshold of $p < 0.05$. STITCH was used to predict metabolite targets; GO and KEGG enrichment of predicted targets was performed. Statistical significance was set at $p < 0.05$ (two-tailed).

3 Results

3.1 Recovery efficiency and calf circumference dynamics under an ERAS protocol

Within an ERAS protocol for heart valve surgery, recovery was efficient: median operation time 6.5 h, ICU stay 44 h, mechanical ventilation 8.9 h. Rehabilitation milestones were early — first limb movement at 14 h, first ambulation at 77.8 h. Median postoperative discharge was 13 days (IQR 4.25 days). Substantial inter-individual variability was observed, particularly in time to ambulation (IQR 69.75 h). These findings support ERAS's potential to accelerate recovery and shorten hospital stays (Table.S1). Against sex-specific cut-offs (men < 34 cm, women < 33 cm),(9) female left calf circumference differed at postoperative and discharge(Table.S3), while female right calf and both male calf measurements were significantly below cut-offs at all time points (all $P < 0.01$). Other limb circumferences are in Table.S2.

3.2 Perioperative Inflammatory and Cardiac Biomarker Dynamics

Perioperative monitoring revealed distinct time-dependent trends. Inflammatory markers peaked postoperatively: CRP rose from 3.95 mg/L preoperatively to 63.34 mg/L postoperatively, remaining elevated at discharge (44.68 mg/L; $\chi^2=24.061$, $p < 0.001$), with hs-CRP showing a similar pattern. Myocardial injury markers increased significantly: CK from 68.00 to 499.00 U/L and CK-MB from 13.00 to 32.00 U/L (both $p < 0.001$). NT-proBNP remained persistently elevated above the normal reference (< 125 pg/mL) across all three time points ($p = 0.856$), reflecting ongoing hemodynamic stress from underlying valvular pathology rather than acute decompensation (Table S4).

3.3 Untargeted Urinary Metabolomics Links to Muscle Loss

QC confirmed high repeatability (78.01% positive, 92.83% negative metabolites with peak-intensity RSD < 30%). Following PQN normalization with osmolality verification, untargeted metabolomics identified 2,533 metabolites in HILIC ESI + and 1,463 in C18 ESI-. PLS-DA models showed good fit and predictive ability (positive: $R^2X = 0.315$, $R^2Y = 0.978$, $Q^2=0.773$; negative: $R^2X = 0.366$, $R^2Y = 0.918$, $Q^2=0.813$); 200-time permutation testing ruled out overfitting (Q^2 intercepts − 0.55 and − 0.45). Using FC > 1.5 or < 0.67, paired t-test $p < 0.05$, and VIP > 1, we identified 234 differential metabolites (107 up, 127 down) in positive mode and 202 (43 up, 159 down) in negative mode. Upregulated signals reflected xenobiotic detoxification, oxidative stress/inflammation, amino acid catabolism, and lipid-carbohydrate dysregulation; downregulated signals included antioxidant flavonoids, bile acid intermediates, and pro-resolving lipid mediators.(10) Upregulated signals reflected xenobiotic detoxification, oxidative stress/inflammation, amino acid catabolism, and lipid–carbohydrate dysregulation; downregulated signals included antioxidant flavonoids, bile acid intermediates, and pro-resolving lipid mediators.

(Table.2, Fig. 1) After excluding drug-derived features, KEGG enrichment ($P < 0.05$) highlighted 21 pathways spanning amino acid, lipid, cofactor/vitamin, and bile acid/gut-liver metabolism. (Table.3) Spearman correlation between postoperative urinary metabolome and discharge calf circumference revealed 20 metabolites significantly associated with muscle loss (average $|r|>0.38$, combined $p < 0.05$), among which acacetin 7-glucuronide ($|r|=0.4558$, $p = 0.0008$) and gravacridonechlorine ($|r|=0.4500$, $p = 0.0010$) showed the strongest positive correlations, whereas glycitein ($|r|=0.4130$, $p = 0.0026$) and pummeline ($|r|=0.4127$, $p = 0.0030$) were negatively correlated.(Table.S5)

3.4 Metabolite-Gene-Pathway Mechanisms of ICU-AW

STITCH predicted targets of 20 significant metabolite-calf circumference correlates, yielding 31 candidate hub genes (associative, not causal). GO terms implicated ossification, immobilization/hypoxia/oxidative stress response, fatty acid metabolism, and skeletal muscle remodeling; KEGG analysis identified 87 pathways, notably endocrine resistance, lipid and atherosclerosis, PI3K-Akt, FoxO, HIF-1 signaling, and steroid hormone biosynthesis. Collectively, these enrichments converge on hypoxia, oxidative stress, inflammatory recruitment, hormonal/lipid metabolic reprogramming, and the PI3K-Akt/FoxO axis, providing a *candidate* mechanistic framework for ICU-associated skeletal muscle loss in cardiac valvular disease patients. (Fig. 2, Table.S6)

4 Discussion

4.1 The "sarcopenia–inflammation–metabolic rewiring" triad in valve surgery

ICU-AW arises from inflammation, immobilization, and metabolic disturbances, driving skeletal muscle catabolism, preferential myosin loss, and mitochondrial impairment.(4, 11) ERAS counters this via early mobilization–activated PI3K/Akt/mTOR anabolism and opioid-sparing analgesia.(12) However, ERAS efficacy is fundamentally constrained by baseline physiological reserve. In patients with severe preoperative sarcopenia, depleted anabolic reserve renders even optimized ERAS insufficient against cardiopulmonary bypass–induced catabolic surge. Thus, ICU-AW should be reframed not as ERAS failure but as a dynamic biomarker of unmet physiological need. Future ERAS must evolve toward precision medicine—integrating objective biomarkers (handgrip dynamometry, quadriceps ultrasonography) with preoperative prehabilitation (resistance training, leucine-enriched nutrition, potential myostatin inhibitors) and physiology-driven mobilization guided by real-time hemodynamic and wearable data,(13) establishing adaptive, resilience-centered ecosystems to reduce ICU-AW burden.

Universal reduction in calf circumference below sex-specific sarcopenia thresholds suggests valvular patients enter surgery with pre-existing sarcopenia — a chronic catabolic state driven by inflammation, malnutrition, and deconditioning.(4, 14) This baseline, compounded by primed ubiquitin-proteasome and autophagic degradation, renders skeletal muscle exquisitely susceptible to surgical catabolic drive, making preferential myosin heavy chain loss and critical illness myopathy highly probable.(15)

Diaphragmatic dysfunction, prolonged ventilation, and failure to mobilize thus reflect preoperative physiological deficit rather than ERAS failure. Asymmetric inter-limb wasting illustrates how iatrogenic factors — invasive lines, chest tubes — actively modulate the pathophysiology of muscle wasting. Even minimal contraction provides an anabolic stimulus, whereas complete immobilization accelerates catabolism. (13)

4.2 Cardiac Recovery vs Persistent Inflammation-Induced ICU-AW

Following heart valve surgery, cardiac functional recovery proceeds reversibly, while skeletal muscle undergoes progressive catabolism. Cardiopulmonary bypass triggers a systemic inflammatory response—C-reactive protein and pro-inflammatory cytokines (IL-6, TNF-α, IL-1β) surge markedly and remain elevated well beyond the early postoperative window, persisting to discharge. (16)In valve surgery, CK/CK-MB show early monophasic rise then decline, mirroring reversible LV dysfunction; NT-proBNP remains elevated, reflecting valvular pathology and hemodynamic loading rather than acute decompensation. Myocardial function recovers spontaneously, while systemic inflammatory drive persists—a clear dissociation.(17) Persistent inflammation drives ubiquitin–proteasome and autophagy-mediated myosin loss and type II fiber atrophy—hallmarks of critical illness myopathy—while causing microvascular, mitochondrial, and oxidative damage. With depleted anabolic reserves in sarcopenia, ICU-acquired weakness becomes deterministic.(18, 19)

ICU-AW should be reconceptualized as an independent organ dysfunction—analogous to acute kidney injury within multiple organ dysfunction syndrome—not merely a consequence of hemodynamic compromise.(2) Normalized cardiac output and recovering LVEF are misleading; persistent inflammation determines muscle wasting and long-term function.(19, 20) Perioperative management must transcend cardiac-centric monitoring to control systemic inflammation and preserve musculoskeletal integrity. ERAS emphasizing early mobilization, optimized nutrition, and proactive anti-inflammatory strategies represents the evolution toward precision perioperative care.

4.3 Perioperative metabolic rewiring reveals actionable nutritional targets

Perioperative VHD surgery triggers multisystem metabolic rewiring. Exercise rehabilitation diverged substantially from controls, coordinately downregulating anti-inflammatory lipid mediators (PGE1, protectin D1) and bile-acid derivatives, reflecting attenuated inflammatory drive and active resolution. Estradiol dropped markedly, indicating HPA-axis activation and surgical catabolism. Conversely, N-desmethylrosiglitazone rose dramatically, signaling exercise-induced CYP450 changes and accelerated biotransformation of lipid-soluble xenobiotics—a pharmacometabolic readout of hepatic clearance plasticity. These shifts frame exercise as a systems-level metabolic organizer recalibrating postoperative homeostasis across lipid/amino acid utilization, oxidative-inflammatory signaling, and endogenous/xenobiotic clearance.(21)

Hydroxyproline-linked dipeptides denote ECM turnover around healing valvular/pericardiac structures; control attenuation of peptide/amino-acid nodes fits persistent catabolic–constrained anabolism. Rising quinolinic acid reflects surgical-stress tryptophan→kynurenine flux; exercise promotes peripheral kynurenine aminotransferase buffering.(22) Acetaminophen mercapturate enrichment reports GST–GSH conjugation and hepatic phase II reserve; polyphenol-conjugate depletion reflects fasting/gut stasis and antioxidant consumption, shifting to Nrf2-driven defence. (23, 24) The 7-ethoxyresorufin signal is likely an annotation artifact. Lidocaine fell to 0.0016-fold, consistent with post-bypass hepatic perfusion restoration;(25) iomeprol trace levels reflect renal washout.(26) Tolcapone is a probable database misassignment requiring MS/MS confirmation.

Peri-operative perturbations in tryptophan, histidine, and vitamin B6 metabolism establish a self-perpetuating "metabolism–inflammation–muscle degradation" cycle.(27) Inflammatory stress diverts tryptophan from serotonin and NAD^+ synthesis toward kynurenine production, thereby depleting substrate for muscle protein synthesis and impairing mitochondrial bioenergetics. Histidine deficiency disrupts carnosine biosynthesis, compromising antioxidant defence, while pyridoxal phosphate deficiency hinders branched-chain amino acid catabolism and creates an energetic bottleneck.(28, 29) Consequent NAD^+ insufficiency cripples cellular energy production; compromised mitochondria become major reactive oxygen species (ROS) sources, hyperactivating inflammatory cascades and manifesting as ICU-acquired weakness (ICU-AW) with prolonged recovery.(30) Metabolite profiles correlated with calf circumference — a validated surrogate of skeletal muscle mass. Seven key metabolites revealed discrete causal chains: quinolinic acid accumulation suggested compensatory NAD^+ salvage activation under inflammatory stress; elevated acacetin 7-glucuronide implied saturated intrinsic clearance;(31) downregulated daidzein coupled with upregulated sulfated metabolites and depleted glycitein signalled gut micro-ecological disturbance neutralising dietary phytoestrogen benefit; and the strongly inverse correlation of metyrosine with calf circumference provided direct molecular evidence that sustained sympathetic–adrenal medullary axis activation drives overt muscle atrophy. These peri-operative metabolic perturbations carry direct nutritional implications. The diversion of tryptophan toward kynurenine suggests that peri-operative NAD^+ precursor supplementation (e.g., nicotinamide riboside) may merit investigation. Histidine deficiency and the consequent compromise of antioxidant defence point to carnosine or β-alanine supplementation as candidate adjuncts. Pyridoxal phosphate deficiency and the resulting bottleneck in branched-chain amino acid catabolism may be amenable to peri-operative pyridoxine repletion. Additionally, the strong inverse correlation of metyrosine with calf circumference suggests that modulation of neuroendocrine tone represents a complementary therapeutic target. Collectively, these metabolic axes delineate putative targets for precision nutritional prehabilitation in cardiac valve surgery patients.

Perioperative exercise in VHD patients reshapes postoperative metabolic architecture—maintaining hepatic GSH–GST detoxification reserve, contracting CPB-driven inflammatory eicosanoid and bile-acid signals, promoting connective-tissue remodelling, and recalibrating the neuroendocrine axis. Disrupted tryptophan/histidine/vitamin B6 metabolism, gut dysbiosis, and neuroendocrine exhaustion lock mitochondria and antioxidant defences into a self-reinforcing inflammatory–proteolytic cycle, driving

skeletal muscle loss and ICU-acquired weakness. Since discrete urinary metabolites correlate with calf circumference, they hold promise as non-invasive muscle-loss biomarkers. Precision ERAS should integrate metabolomic phenotyping to target the microbiome–NAD^+–neuroendocrine axis and protect skeletal muscle during recovery.

4.4 Mechanisms of ERAS-Resistant Atrophy in Valve Surgery

Despite ERAS-guided training, valve surgery patients still showed reduced muscle circumference. Enrichment analysis revealed a pathological network—inflammation, hypoxia, oxidative stress, endocrine resistance, apoptosis—that suppressed exercise-induced anabolic signaling, producing net catabolism. (32) IL-6/TNF-α activate NF-κB and FoxO, upregulating the ubiquitin–proteasome system (Atrogin-1, MuRF1) to accelerate proteolysis. Concurrently, ROS accumulation impairs mitochondrial integrity, lowering ATP, activating AMPK, and suppressing mTORC1—blocking exercise-induced protein synthesis. These converging mechanisms override ERAS benefits, driving ICU-AW. (33)

Valvular heart disease causes hypoxia, activating HIF-1α to shift muscle metabolism toward inefficient glycolysis, blunting PI3K-Akt signaling and exercise responsiveness. (34, 35) Concurrently, endocrine resistance emerges—impaired sex hormone transduction reduces PI3K-Akt/mTOR-mediated protein synthesis, while stress-induced hypercortisolism activates glucocorticoid receptor–FoxO signaling, upregulating Atrogin-1/MuRF1 and driving proteasome- and autophagy-mediated breakdown.(32, 36) These converging pathologies suppress exercise-induced anabolic signaling, explaining why ERAS-guided training fails to prevent net protein catabolism and muscle circumference reduction. PI3K-Akt is the central hub of muscle homeostasis. Under postoperative stress, inflammatory cytokines and oxidative stress suppress Akt, releasing FoxO3 to upregulate CASP3 and apoptosis.(37, 38) Elevated MMP2/9 degrade type IV collagen and perimysial ECM, compromising structural integrity. ICU confinement imposes immobilization stress. Although ERAS emphasizes early mobilization, actual activity rarely reaches the threshold to counteract systemic catabolism. Amino acids from muscle breakdown are redistributed to acute-phase protein synthesis and wound healing—a "muscle-to-central-tissue" metabolic cost that perpetuates net protein loss.

Inflammation, hypoxia, oxidative stress, endocrine resistance, and apoptosis suppress PI3K-Akt/mTOR and activate FoxO-mediated proteolysis in valve surgery patients, so ERAS exercise alone cannot reverse atrophy; multimodal strategies are required.

4.5 Toward precision nutritional prehabilitation in valve surgery

Persistent lower-limb circumference loss reflects perioperative catabolism — systemic inflammation, surgical trauma, and immobility — overwhelming standard anabolic stimuli, especially with preoperative sarcopenia. This tips protein turnover toward catabolism, manifesting as the muscle-wasting phenotype that elevates ICU-AW risk. Closing the gap between ERAS and physiological resilience demands a "heart-

muscle synergy" paradigm: (i) preoperative prehabilitation targeting protein synthesis (high-dose protein, leucine, vitamin D) and the tryptophan/histidine/vitamin B6 axes; (ii) intraoperative refinement to minimize cardiopulmonary bypass-induced inflammatory surge; (iii) postoperative rehabilitation guided by physiology and metabolomic phenotyping. The 20 calf circumference-correlated metabolites are *putative* non-invasive biomarkers warranting validation in larger controlled cohorts with concurrent MRC sum score assessment and targeted LC-MS/MS quantification.

5 Conclusion

This prospective exploratory study provides the first integrated characterization of occult muscle wasting and urine metabolomic reprogramming in ERAS-guided valve surgery. Three perturbated metabolic axes — tryptophan, histidine, and vitamin B6 — emerge as candidate targets for precision nutritional prehabilitation. The 20 metabolites correlating with calf circumference are *putative* non-invasive biomarkers of the muscle-wasting phenotype overlapping with ICU-AW risk, requiring validation in larger controlled cohorts with MRC sum score assessment and targeted LC-MS/MS. Future studies should incorporate a contemporaneous non-ERAS arm, expand metabolomics to n ≥ 80, and integrate MRC sum score with bedside ultrasound to formally diagnose ICU-AW and partition fluid from lean-tissue loss. Given the vulnerability of urine metabolomics to hydration effects, osmolality correction or raw-plus-normalized reporting is essential to avoid erroneous conclusions.

Declarations

Ethical approval

This prospective observational study was approved by the Medical Ethics Committee of The First Hospital of Lanzhou University (No. LDYYLL2026-526) and conducted per the Declaration of Helsinki with written informed consent from all participants.

Funding

This research did not receive any specific grant from funding agencies in the public, commercial, or not-for-profit sectors.

Conflict of Interest

The authors declare no conflicts of interest.

Acknowledgements

We appreciate the cardiovascular surgery team and patients at The First Hospital of Lanzhou University, and colleagues at Shanghai University of Sport for their contributions to data collection and analysis.

Author contributions (CRediT):

Chengyao Xu: Conceptualization, Writing – original draft, Investigation.

Shidong Liu: Methodology, Formal analysis, Validation.

Dan Guo: Investigation, Data curation.

Haiyi He: Formal analysis, Visualization.

Bing Song: Supervision, Project administration, Funding acquisition.

Xin Xu: Conceptualization, Project administration, Writing – review & editing, Supervision.

Data availability

Raw metabolomics data are deposited in OMIX (accession: OMIX016728). Additional data supporting the findings of this study are available from the corresponding author upon reasonable request.

Declaration of Generative AI

The authors did not use generative AI in the writing of this manuscript.

References

1. Vanhorebeek, I., Latronico, N. & Van den Berghe, G. ICU-acquired weakness. *Intensive Care Med.* **46** (4), 637–653 (2020).
2. Huang, A. et al. ICU-acquired weakness: Critical illness myopathy and polyneuropathy. *J. Crit. Care*. **88**, 155074 (2025).
3. Inoue, S. et al. Post-intensive care syndrome: Recent advances and future directions. *Acute Med. Surg.* **11** (1), e929 (2024).
4. Lad, H. et al. Intensive Care Unit-Acquired Weakness: Not just Another Muscle Atrophying Condition. *Int. J. Mol. Sci.* ;**21**(21). (2020).
5. Fazzini, B. et al. The rate and assessment of muscle wasting during critical illness: a systematic review and meta-analysis. *Crit. Care*. **27** (1), 2 (2023).
6. Le Stang, V., Latronico, N., Dres, M. & Bertoni, M. Critical illness-associated limb and diaphragmatic weakness. *Curr. Opin. Crit. Care*. **30** (2), 121–130 (2024).
7. Shin, S. Y. et al. An atlas of genetic influences on human blood metabolites. *Nat. Genet.* **46** (6), 543–550 (2014).
8. Rousseau, A. F. et al. Serum Acylcarnitines Profile in Critically Ill Survivors According to Illness Severity and ICU Length of Stay: An Observational Study. *Nutrients* ;**15**(10). (2023).
9. Portero-McLellan, K. C. et al. The use of calf circumference measurement as an anthropometric tool to monitor nutritional status in elderly inpatients. *J. Nutr. Health Aging*. **14** (4), 266–270 (2010).

10. Triba, M. N. et al. PLS/OPLS models in metabolomics: the impact of permutation of dataset rows on the K-fold cross-validation quality parameters. *Mol. Biosyst*. **11** (1), 13–19 (2015).
11. Othman, S. Y., Elbiaa, M. A., Mansour, E. R., El-Menshawy, A. M. & Elsayed, S. M. Effect of neuromuscular electrical stimulation and early physical activity on ICU-acquired weakness in mechanically ventilated patients: A randomized controlled trial. *Nurs. Crit. Care*. **29** (3), 584–596 (2024).
12. Coleman, S. R. et al. Enhanced Recovery Pathways for Cardiac Surgery. *Curr. Pain Headache Rep.* **23** (4), 28 (2019).
13. Licker, M. et al. Multi-Modal Prehabilitation in Thoracic Surgery: From Basic Concepts to Practical Modalities. *J. Clin. Med.* ;**13**(10). (2024).
14. Lippi, L. et al. Efficacy of Physiotherapy Interventions on Weaning in Mechanically Ventilated Critically Ill Patients: A Systematic Review and Meta-Analysis. *Front. Med. (Lausanne)*. **9**, 889218 (2022).
15. Mendelson, A. A., Erickson, D. & Villar, R. The role of the microcirculation and integrative cardiovascular physiology in the pathogenesis of ICU-acquired weakness. *Front. Physiol.* **14**, 1170429 (2023).
16. Tian, H. et al. Preoperative inflammatory markers predict postoperative clinical outcomes in patients undergoing heart valve surgery: A large-sample retrospective study. *Front. Immunol.* **14**, 1159089 (2023).
17. Dépret, F. et al. Esophageal Doppler Can Predict Fluid Responsiveness Through End-Expiratory and End-Inspiratory Occlusion Tests. *Crit. Care Med.* **47** (2), e96–e102 (2019).
18. Zanders, L. et al. Sepsis induces interleukin 6, gp130/JAK2/STAT3, and muscle wasting. *J. Cachexia Sarcopenia Muscle*. **13** (1), 713–727 (2022).
19. Chen, J. & Deng, Y. Diagnostic Performance of Serum CK-MB, TNF-α and Hs-CRP in Children with Viral Myocarditis. *Open. Life Sci.* **14**, 38–42 (2019).
20. Zhang, X. et al. Risk Factors, Diagnostic Challenges, and Emerging Therapeutic Strategies for ICU-Acquired Weakness: A Brief Review. *J. Multidiscip Healthc.* **18**, 7769–7778 (2025).
21. Lu, C. et al. Comprehensive metabolomic characterization of atrial fibrillation. *Front. Cardiovasc. Med.* **9**, 911845 (2022).
22. Jaguri, A., Al Thani, A. A. & Elrayess, M. A. Exercise Metabolome: Insights for Health and Performance. *Metabolites* ;**13**(6). (2023).
23. Fei, W. et al. Antioxidative and Energy Metabolism-Improving Effects of Maca Polysaccharide on Cyclophosphamide-Induced Hepatotoxicity Mice via Metabolomic Analysis and Keap1-Nrf2 Pathway. *Nutrients* ;**14**(20). (2022).
24. Zhang, H. et al. Pre-operative exercise therapy triggers anti-inflammatory trained immunity of Kupffer cells through metabolic reprogramming. *Nat. Metab.* **3** (6), 843–858 (2021).

25. Olkowicz, M. et al. Preoperative untargeted SPME-LC/HRMS-based metabolomic profiling in cardiac surgical patients identified prognostic biomarkers for postoperative outcomes. *Anal. Chim. Acta*. **1383**, 344900 (2026).
26. Mao, H. et al. High preoperative blood oxaloacetate and 2-aminoadipic acid levels are associated with postoperative delayed neurocognitive recovery. *Front. Endocrinol. (Lausanne)*. **14**, 1212815 (2023).
27. Ahmed, N. et al. Metabolic Changes in Early-Stage Non-Small Cell Lung Cancer Patients after Surgical Resection. *Cancers (Basel)* ;**13**(12). (2021).
28. Grunow, J. J. et al. Muscular myostatin gene expression and plasma concentrations are decreased in critically ill patients. *Crit. Care*. **26** (1), 237 (2022).
29. Chang, Y. et al. Metabolic Characteristics and Discriminative Diagnosis of Growth Hormone Deficiency and Idiopathic Short Stature in Preadolescents and Adolescents. *Molecules* ;**29**(7). (2024).
30. Klawitter, F., Ehler, J., Bajorat, R. & Patejdl, R. Mitochondrial Dysfunction in Intensive Care Unit-Acquired Weakness and Critical Illness Myopathy: A Narrative Review. *Int. J. Mol. Sci.* ;**24**(6). (2023).
31. Lu, Z. et al. ATF3 and CH25H regulate effector trogocytosis and anti-tumor activities of endogenous and immunotherapeutic cytotoxic T lymphocytes. *Cell. Metab.* **34** (9), 1342–58e7 (2022).
32. Tarum, J., Ball, G., Gustafsson, T., Altun, M. & Santos, L. Artificial neural network inference analysis identified novel genes and gene interactions associated with skeletal muscle aging. *J. Cachexia Sarcopenia Muscle*. **15** (5), 2143–2155 (2024).
33. Chen, J., Zhou, R., Feng, Y. & Cheng, L. Molecular mechanisms of exercise contributing to tissue regeneration. *Signal. Transduct. Target. Ther.* **7** (1), 383 (2022).
34. Sun, K. et al. The Use of Identified Hypoxia-related Genes to Generate Models for Predicting the Prognosis of Cerebral Ischemia–reperfusion Injury and Developing Treatment Strategies. *Mol. Neurobiol.* **62** (3), 3098–3124 (2025).
35. Chen, H. et al. Exercise training maintains cardiovascular health: signaling pathways involved and potential therapeutics. *Signal. Transduct. Target. Ther.* **7** (1), 306 (2022).
36. Hu, Y. et al. Passive exercise is an effective alternative to HRT for restoring OVX induced mitochondrial dysfunction in skeletal muscle. *Front. Endocrinol. (Lausanne)*. **15**, 1356312 (2024).
37. Zhou, Y., Zhang, X., Baker, J. S., Davison, G. W. & Yan, X. Redox signaling and skeletal muscle adaptation during aerobic exercise. *iScience* **27** (5), 109643 (2024).
38. Hu, K. et al. Identification and Validation of PTGS2 Gene as an Oxidative Stress-Related Biomarker for Arteriovenous Fistula Failure. *Antioxid. (Basel)* ;**13**(1). (2023).

Tables

Table.1 Baseline Demographic and Clinical Characteristics of the Study Cohort Height

Age(Y)	Type	M(P25,P75)/N,%
	56.00(47.00, 63.00)	
Gender	Male	50,54.2%
	Female	43,45.8%
Hight(m)		1.67(1.60, 1.72)
Weight(kg)		62.00(54.00, 74.00)
BMI		22.27(20.38, 25.72)
Euro-SCORE		1.83(0.72, 2.38)
NYHA functional class	I	8,8.75%
	II	59,62.50%
	III	2,28.75%

Table.2 Differential metabolites

KEGG ID	Name	P value	FDR	Fold Change	VIP
C09364	Bicuculline	5.64E-04	6.49E-03	0.50	1.90
C07706	Perindopril	1.54E-04	2.46E-03	1.50	1.87
C14536	Glycitein	8.97E-04	8.63E-03	2.50	1.86
C10208	Daidzein	5.67E-04	6.50E-03	3.50	1.84
C17726	beta-muricholic acid	3.42E-04	4.44E-03	4.50	1.84
C08716	Malvidin	3.07E-04	4.07E-03	5.50	1.83
C07921	Metyrosine	4.75E-04	5.64E-03	13.78	1.83
C07814	Homatropine	1.02E-04	1.81E-03	0.13	1.81
C06563	Genistein	3.17E-04	4.19E-03	0.24	1.80
C10842	Anisodamine	1.40E-04	2.27E-03	175.77	1.77

Table.3 Differential metabolic pathways

Pathway code	Pathway	Hits	p Value	FDR
hsa00232	Caffeine metabolism	2/22	7.30E-03	0.088
hsa00380	Tryptophan metabolism	3/83	1.25E-02	0.088
hsa00750	Metabolism of vitamin B6	2/29	1.25E-02	0.088
hsa04977	The digestion and absorption of vitamins	2/42	2.53E-02	0.131
hsa00340	Histidine metabolism	2/47	3.12E-02	0.131
hsa04960	Aldosterone-regulated sodium reabsorption	1/8	4.67E-02	0.163
hsa05224	breast cancer	1/3	4.74E-03	0.062
hsa01522	Endocrine drug resistance	1/5	7.88E-03	0.062
hsa04915	Estrogen signaling pathway	1/8	1.26E-02	0.062
hsa04961	Calcium reabsorption regulated by endocrine and other factors	1/8	1.26E-02	0.062

Figures

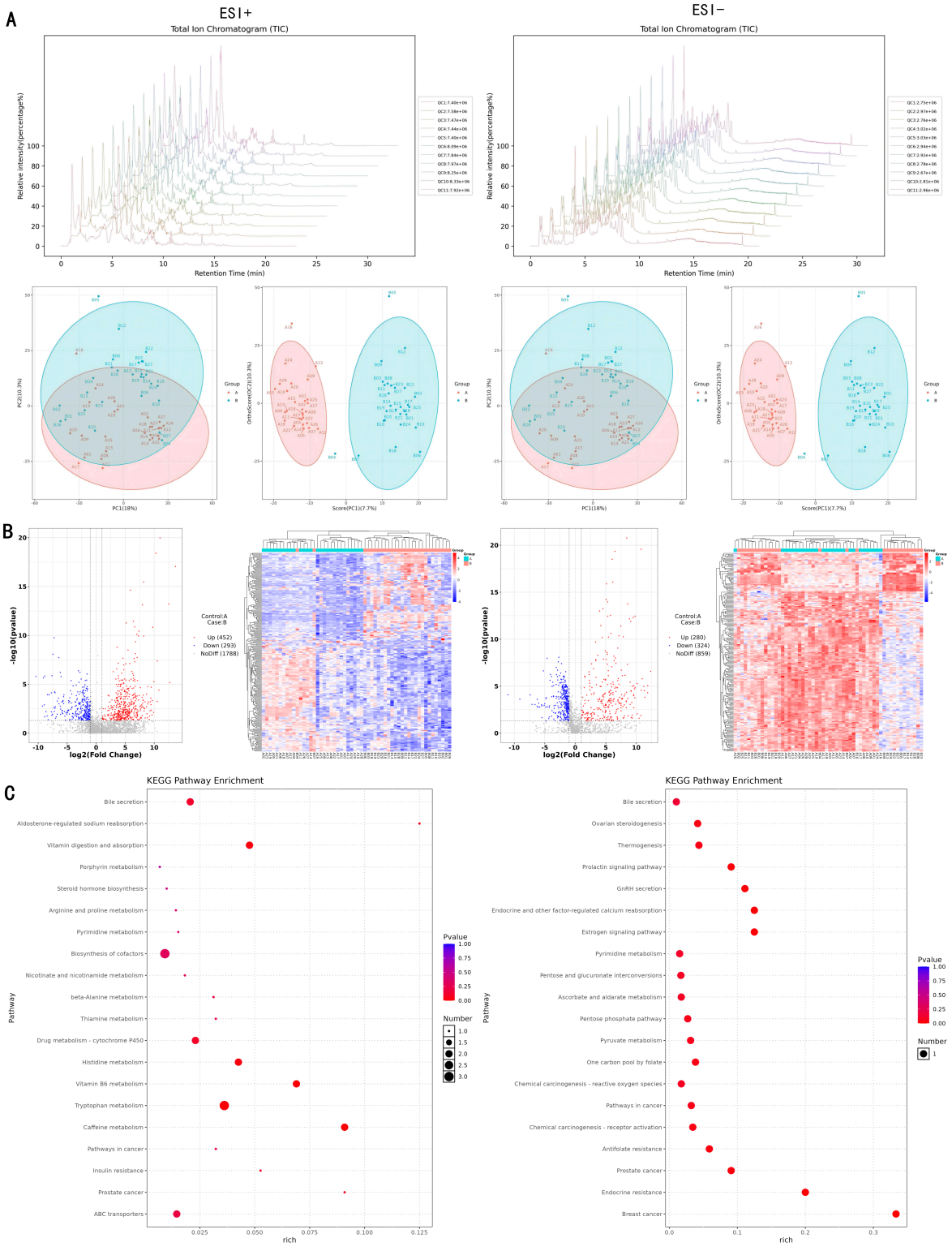


Figure 1

Legend not included with this version.

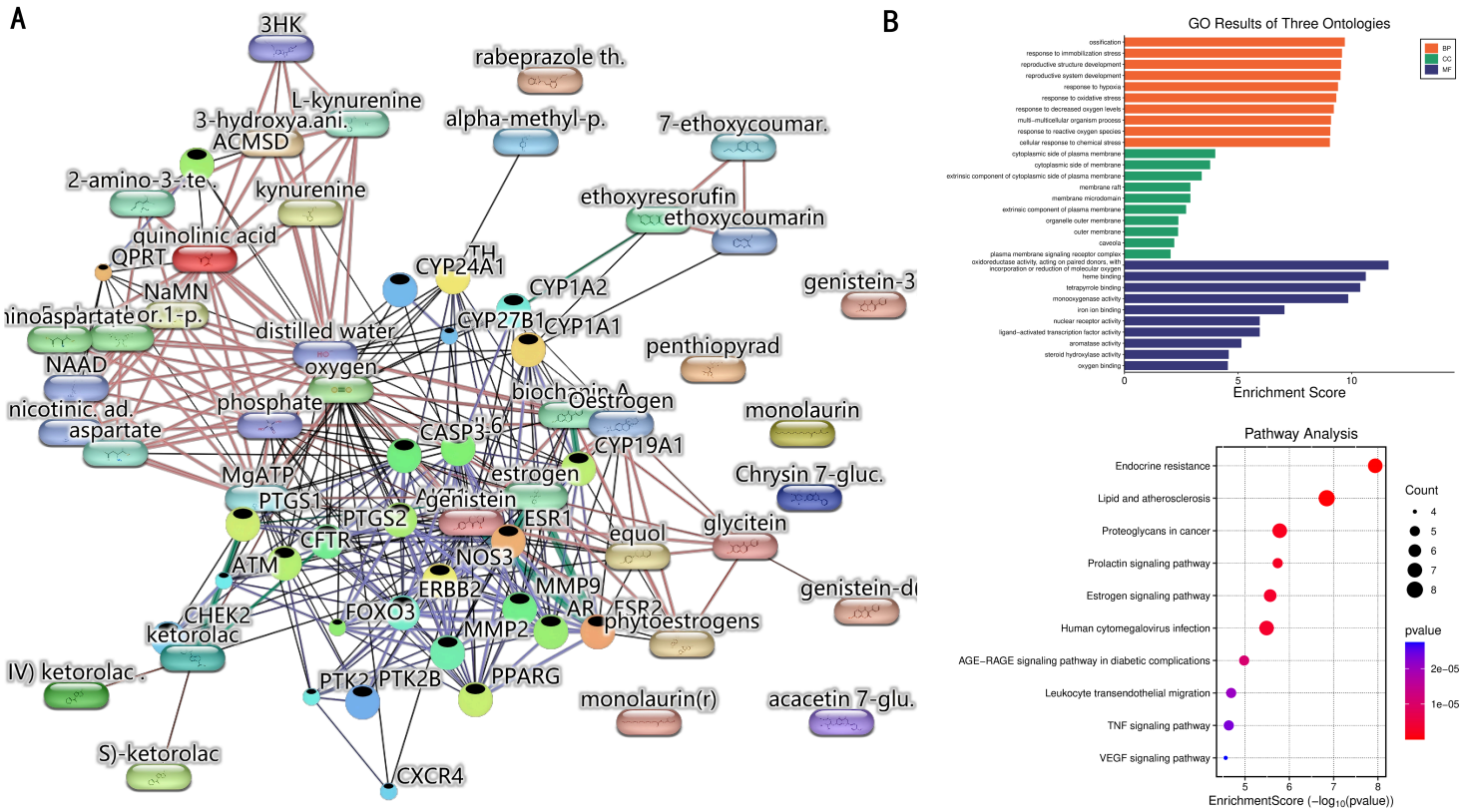


Figure 2

Legend not included with this version.

Supplementary Files

This is a list of supplementary files associated with this preprint. Click to download.

- Supplementarymaterials.docx